FIRST STEREOSCOPIC RADAR IMAGES OF TITAN. R. L. Kirk[1], E. Howington-Kraus[1], K. L. Mitchell[2], S. Hensley[2], B. W. Stiles[2] and the Cassini RADAR Team, [1]U.S. Geological Survey, Asgtrogeology Program, Flagstaff, AZ 86001 (rkirk@usgs.gov), [2]Jet Propulsion Laboratory, Pasadena, CA 91109.

Introduction: The T18 flyby of Titan on 23 September 2006 marked a watershed in the operation of the Cassini RADAR instrument [1]. The seven synthetic aperture radar (SAR) images obtained on earlier flybys all covered non-overlapping areas of Titan's surface. (High altitude SAR images obtained beginning with T13 overlaps the standard SAR images, but their spatial resolution is lower, making the kinds of analyses reported here problematic.) In contrast, image swaths from T18 to the end of the prime mission, with only a single exception, overlap at least one prior image. The repeat coverage obtained so far includes T18 and T19 images of part of the T16 swath with same-side and opposite-side geometry, respectively, and a nearly orthogonal crossing of T8 by T21. Shortly after this is written, T23 will provide an opposite-side view of Ta, including the putative cryovolcanic dome Ganesa. Subsequent overlaps will include nearly every possible combination of the passes in the series T25-28-29-30 with those in the set Ta-3-16-18-19-21-23, which cross the northern hemisphere almost orthogonally to the first group, as well as more widely distributed pairs at the end of the prime mission. The overlapping image coverage will be useful for multiple types of study, as follows

Geodetic control. The RADAR SAR images already serve as the reference for geolocating optical images, because the positions of the latter are susceptible to pointing errors but those of the former are not. Measurements of features in a dense, near-global (with extended mission coverage) set of overlapping SAR swaths will provide the basis for further improving their positional accuracy, and possibly for determining the spin axis of Titan with sufficient precision to discriminate between models of its interior structure.

Scattering properties. The dependence of radar backscatter on both incidence angle and illumination direction provides clues to wavelength-scale texture, composition, layering, and surface slopes.

Change detection. Evidence for surface change may be ambiguous in the face of the other effects listed here, but the RADAR will provide the highest resolution images of Titan with a time base of weeks to years and hence the best chance of documenting such activity.

Topographic mapping. Matching features between images provides information about the absolute and relative relief at comparatively high horizontal resolution, on the order of 1 km. Such matching is challenging because speckle noise, differences in image resolution and quality, and illumination differences (especially illumination from opposite sides) can result in images that look quite different.

In this abstract, we describe preliminary efforts to derive topographic information from the T16-18, 16-19, and 8-21 image pairs. Updated results, and first results for T23-Ta, will be shown in our poster. A companion abstract [2] describes models of the radar scattering properties of putative methane lakes [ref] in the T16-19 overlap.

Background—Titan's Topography: Stereoanalysis of images from the Huygens probe revealed relief of 150-250 m and slopes up to 30° near the landing point [3] but the resolution of the optical imaging systems on the Cassini orbiter has been inadequate to extend such mapping to broader areas. The bulk of current information about Titan's topography thus comes from the RADAR instrument. Operating in altimeter mode, it yields elevation profiles a few hundred km in length, with a horizontal resolution of 25–40 km and one-way range resolution of 30 m [4]. The first half-dozen profiles show relief of ≤150 m and give an average radius of 2575.5±0.1 km, consistent with the Voyager occultation results of 2575±0.5 km [5]. Tens more profiles are being obtained in the prime mission and may reveal more variety.

Altimetry-like elevation profiles with 200 m vertical and 50 km horizontal resolution have been obtained by innovative processing of the SAR images [6]. Results to date show little variation in height, even over large impact and volcanic features and the continent-sized bright feature Xanadu, though this may be a result of the limited resolution of the method. Radarcliometry (or shape-from-shading) has been applied to the images to estimate heights of features down to the image resolution (a few hundred m). Early results suggested possible cryovolcanic flows [7] and mountains [8] had low relief of only 100–300 m. Estimates of the height of mountains were later revised upward by ~50% based on reassessment of the probable scattering law, and mountains with inferred heights exceeding 1 km were found to be ubiquitous in Xanadu and some other areas [9,10]. Radarclinometry-derived heights for dunes in the equatorial "sand seas" were found to be 100–150 m, comparable to dunes of similar form on Earth [11].

Thus, the information to date suggests that Titan is a world of subdued relief, with local topography typically a few hundred meters or less and only occasionally exceeding 1 km. The radarclinometry results, in particular, need to be checked at least locally by other methods such as stereo, because the technique is so dependent on the scattering model assumed.

Methodology: The ultimate goal is to use a physically rigorous sensor model to estimate the 3D coordinates of each stereo match point. Researchers at JPL are modiying their Magellan based stereo tools, while the ultimate goal of the USGS is to adapt their commercial photogrammetric workstation to work with Cassini RADAR data. Until this capability becomes available, however, we are able to estimate relative and even absolute heights (with a higher degree of uncertainty) based on measurements of parallax between images and a simplified conversion from parallax to height. A point with height h relative to the reference surface will be displaced from its true horizontal location by a parallax $p = h \cot(i)$ when a radar image with incidence angle i is georeferenced to that flat surface. The height that corresponds to a net parallax of one pixel will therefore be $h / \Delta p = GSD / (\cot(i_1)-\cot(i_2))$ for same-side imaging (where GSD is the ground sample distance in m), $GSD / (\cot(i_1)+\cot(i_2))$ for opposite-side imaging, and $GSD / \sqrt{(\cot^2(i_1)+\cot^2(i_2))}$ for images that cross at right angles [12]. Thus, the opposite-side geometry is most favorable for resolving elevation differences, but is least favorable for comparing the images if they contain both intrinsically dark and bright areas (which appear similar) and topographic shading, which will appear reversed under opposing illumination.

Our measurement of parallax begins with projecting the two images to be compared, each of which is archived in an oblique cylindrical projection tied to its flyby geometry [13] into a common projection. This is achieved with a simple customized resampling tool at JPL, or can be conveniently done in the USGS cartographic software system ISIS (http://isis. astrogeology.usgs.gov), which is freely available to researchers interested in Cassini data. One of the images may be projected to the coordinates of the other, or the two may be transformed to a common system such as polar stereographic (for the T16-18 and 16-19 pairs, which are near-polar and near-parallel) or simple cylindrical (for T8-21, which cross perpendicularly near the equator). The maps of incidence angle for each image may be similarly transformed, and a map of the height per unit parallax (which can vary strongly with location) may be calculated from them, based on the formulae just given.

We have mapped parallax, and thus relative elevation, over the T16-19 pair by applying an area-based automatic matching algorithm originally developed for analysis of Magellan radar images [14]. Matching is done hierarchically, working from coarse to fine matches to track the local parallax differences help eliminate matching errors. Correspondences were obtained at 1/32° (1.4 km) separation but were based on correlation of a 1/4° (11 km) square box; thus, the resulting digital terrain model (DTM) only partly resolves features smaller than 11 km in size. Reducing the size of the matching area would be desirable to improve resolution, but is impractical because of the noise and illumination differences between the images.

In order to estimate the elevations of features of interest at the highest possible resolution, we have therefore resorted to interactive viewing and measurement; the human visual system performs better at stereomatching than even the best current algorithms. Initial comparison of the images is conveniently made in the ISIS display program *qview*, which

allows zooming, panning, and blinking of coregistered images. For more detailed comparison including measurements of parallax, we imported the images (in 8-bit logarithmically scaled form [13]) into Adobe Photoshop. The paired images can be combined either as an anaglyph or as superimposed image layers whose visibility can be turned on and off; in either case, the images can quickly be smoothed to varying extents to reduce the distracting effects of "speckle" noise and can be shifted with respect to one another to determine the mean parallax in a region and visualize variations around this mean. We initially tried to measure parallaxes by recording the coordinates of corresponding points on images either side-by-side or superimposed as layers, but this proved to be extremely challenging. In some areas, we found it useful to enlarge the superimposed images (after smoothing to suppress noise) and trace features such as lake shorelines and scarp crests in each separately, then compare the tracings. This amounts to an interactive version of "feature based" automated matching approaches [15].

Results:

T16-18. The overlap area extends from 35°N 347°W to 53°N 342°W and covers approximately 140x800 km. Incidence angles range from 17–28° in T16 and 25°–43° from the same side in T18, and vary in an opposite sense, so that the height per pixel of parallax (at 1/128° per pixel or 351 m) ranges from 200 m at the southern end of the strip to infinity at 51°N where the incidence angles are equal. Rugged and very interesting terrain unfortunately lies at this point of no stereo convergence. The only other conspicuous, probably topographic, feature is a bright region dissected by dark lanes near 42°N 348°W that broadly resembles mountainous areas elsewhere on Titan [10]. Blinking of the images reveals no more than 1 pixel relative parallax between features in this area, placing an upper limit of ~400 m on local relief. The typical absolute offset between the two images (as georeferenced to the 2575 km sphere) is about 0.6 km across track and 1 km along track, and is presumably an indication of the uncertainty in the reconstructed spacecraft trajectories.

T16-19. The 250x2300 km overlap area extends from ~35°N 148°W to 82°N 84°W. Incidence angles range from 9–39° in T16 and 9–26° (opposite side) in T19 and vary in roughly the opposite sense, so the height per pixel of parallax ranges only from 40–76 m. The absolute along-track offset between the images appears to be 0.3 km (1 pixel) or less, all along the strip. A series of very dark features in steep-sided depressions, interpreted as lakes [16], and similar depressions that do not have dark floors occupy the northern part of the stereopair. The southern end is dominated by what appears to be a large system of canyons, though the image resolutions are poor here. Area-based automatic matching indicates a total elevation range of almost 1000 m, mainly across the width of the strip in the region of the canyon system. Elevation differences of 100–200 m are associated with the lakes, but only the largest of these features exceed the size of the matching patch used.

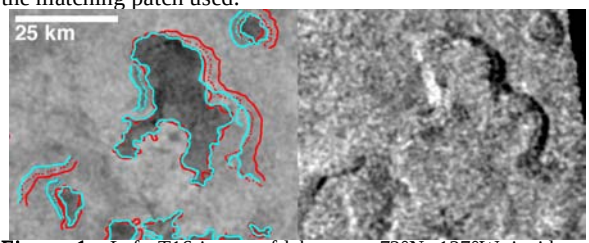

Figure 1. Left, T16 image of lakes near 72°N 127°W, incidence 30°, from left. Shorelines and scarps have been traced in cyan; red traces are same features in T19 image. Right, "magic airbrush" composite (weighted difference) of T16 and T19 images suppresses backscatter variations and reveals subtle slope details.

In the hope of determining elevations at and around the lakes at higher resolution, we measured parallaxes by the interactive methods described above. The majority of the dark lakes have shores that are collocated to one or at most two 0.35-km pixels in the paired images; local fluctuations in the shoreline due to speckle and possible contrast variations (generally less dramatic than those described in [2]) are of this same magnitude and limit the precision with which measurements can be made. These measurements indicate that the lakes are within 50–100 m of the same elevation, and, indeed, within 100 m of the 2575 km reference radius used in georeferencing the images. The similar elevation of the lakes is consistent with (but does not require) their connection to a methane "aquifer" whose "water table" controls their level [16]. A few small lakes and bright-floored depressions near 73°N 125°W appear to be ~250 m above the level of the other lakes, however. The heights of the scarps that bound most depressions are relatively consistent on the east and west margins (the north and south margins are difficult to see). Scarp heights range from a few hundred m for some lakes up to 600 m for a few others. Thus, it would appear that, whereas the depression floors and lakes are mostly on a consistent level, the rims are not This may be evidence that the depressions are constructional in origin, i.e., that they are calderas [17]. Alternatively, the depressions may have been eroded into a relatively undulating surface but filled to a constant level. Visualization of subtle surface relief by "magic airbrush" processing of the images [18] (so named because a shaded-relief-like product is obtained by the "magically" simple approach of taking the weighted difference of the opposite-side images in which intrinsic brightness variations cancel and slope shading is reinforced) seems to support the constructional hypothesis by revealing locally built-up areas around a few of the lakes.

T8-21. These strips overlap at almost a right angle, in the 390x 580 km region 14–5°S, 284–297°W. The version of the T21 image currently available is geolocated based on preliminary spacecraft trajectory and pointing data, and shows a net offset of 10 km and internal distortions on the order of 3 km with respect to T8. We have therefore not yet attempted a detailed comparison, but it is noteworthy that the many dunes identified in T8 [11] are also visible as dark streaks of comparable contrast in T21. The latter image, in which the illumination is along the dunes, does not, however, show the bright edges that were interpreted as radar-facing slopes in the earlier image with illumination across the dunes. This comparison supports both the interpretation of the streaks as dunes and the estimates of their heights obtained by radarclinometry.

Future Work: We are working to complete sensor model software for the Cassini RADAR, to be used in the automatic matching tools developed by JPL and in the SOCET SET (® BAE Systems) digital photogrammetric software package used at USGS [19]. This software will calculate the transformation between image coordinates and Titan ground coordinates based on a physically rigorous model of the imaging process, the best available spacecraft trajectory data, and adjustments to the trajectory chosen to improve the registration between images at a set of measured tiepoints [20]. Using the sensor models, we will "tune" the parameters controlling the very flexible JPL and SOCET automatic matching packages to produce the best possible DTMs. We will also be able to view the images and DTMs on the electro-optical stereo display of the SOCET workstation, in order to interactively edit DTMs or extract three-dimensional coordinates of specific features. Given the challenging properties of the radar stereo images described above, as well as the scientific interest in studying Titan's topography in as much detail as possible, we anticipate that the interactive approach will be especially productive.

References: [1] Elachi, C., et al. (2004) *Space Sci. Rev., 115*, 71. [2] Mitchell, K.L., et al. (2007) this conference. [3] Tomasko, M., et al. (2005) *Nature, 438*, 765; Soderblom, L.A., et al. (2007) *Planet. Space Sci.*, submitted. [4] Callahan, P., et al. (2007) *JGR*, submitted. [5] Lindal, G.F., et al. (1983) *Icarus, 53*, 348. [6] Stiles, B.W., et al. (2006) *AAS Bull., 38*, 57.07. [7] Kirk, R.L., et al. (2005) *LPS, XXXVI*, 2227. [8] Radebaugh, J., et al. (2006) *LPS, XXXVII*, 1007. [9] Kirk, R.L., et al. (2006) *AAS Bull. 38*, 52.03. [10] Radebaugh, J., et al. (2007) *Icarus*, submitted. [11] Lorenz, R.D., et al. (2006) *Science, 312*, 724. [12] Plaut, J.J. (1993) in *Guide to Magellan Image Interpretation*, JPL Pub. 932-24, 33. [13] Stiles, B. (2005) Cassini Radar Basic Image Data Record SIS, JPL D-27889, v. 1.3. [14] Hensley, S. et al., 1994, *IGARSS 94*, 3, 1470. [15] Vosselman, G., et al. (2004) in *Manual of Photogrammetry, 5th Ed.*, 492. [16] Stofan, E., et al. (2007) Nature, 445, 61. [17] Mitchell, K.L., et al. (2006) *AAS Bull. 38*, 52.05; Wood, C., et al. (2006) *AAS Bull. 38*, 52.08; (2007) this conference. [18] Planetary Cartography Working Group (1993) *Planetary Cartography 1993–2003*, NASA, Fig. 3; see Kirk, R.L., et al. (2005) *PE&RS, 71*, 1168, for a detailed explanation of a similar technique using optical data. [19] Miller, S.B., and A.S. Walker (1993) *ACSM/ASPRS Annual Conv., 3*, 256; (1995) *Z. Phot. Fern. 63*, 4.. [20] Howington-Kraus, E., et al. (2000) *LPS, XXXI*, 2061; (2002) *LPS, XXXIII*, 1986.